# Asymptotic Analysis of Three-Dimensional Scattered Field in a Shadow Region of a Convex Cylinder

Toyohiko Ishihara and Tomohiro Sugihara Department of Electrical Engineering, National Defense Academy, Hashirimizu, Yokosuka, 239, Japan

## 1. INTRODUCTION

When an incident wave illuminates the smooth convex surface at the grazing incidence, a part of the energy is carried out into the shadow region by the creeping wave which sheds diffracted rays tangentially from the surface as it propagates. The geometrical theory of diffraction (GTD) has been developed by Keller<sup>[1],[2]</sup> to describe this diffraction phenomenon. However, the GTD fails in the transition region near the shadow boundary (SB). A uniform GTD (UTD) has been developed by Pathak, Burnside, and Marhefka<sup>[3]</sup> which remains valid in the transition region, and which reduces to the original GTD in the deep shadow region. The UTD formulation contains the Fresnel integral as the transition function and the Pekeris caret function that reduces to the GTD. The UTD has been widely used in calculating the radiated fields of antennas mounted near curved surfaces. Recently, Hussar and Albus<sup>[5]</sup> compared the UTD with the exact eigenfunction solution and found that the UTD becomes inaccurate in the deep shadow region. The UTD does not reduce to the original GTD in the deep shadow region since the Fresnel integral does not approach unity fast enough.

In this paper, we begin with the analysis of the diffraction field by perfectly conducting circular cylinder due to an electric or a magnetic line source located sufficiently away from the convex surface. We derive the modified GTD solution from the exact residue series solution<sup>[6]</sup>. The analysis is generalized to the three-dimension by considering the diffraction field excited by a point source. Because of a simple Fourier integral relation that connects two-dimensional and three-dimensional Green's functions, the results due to the line source excitation can be utilized directly<sup>[6]</sup>. The utility and validity of the asymptotic representations involving the GTD, the UTD, and the modified GTD are assessed by numerical calculations.

## 2. ANALYTICAL FORMULATION

## 2.1 Two-dimensional problem due to a line source

The canonical problem of the diffraction field by an infinitely long circular cylinder is examined in this section. The geometry of the two-dimensional problem is shown in Fig.1. The two-dimensional Green's function  $\overline{G}_{s,h}(\tilde{\rho},\tilde{\rho}',k)$  at the point  $P(\tilde{\rho})$ ,  $\tilde{\rho}=(\rho,\phi)$ , excited by an electric or a magnetic line source  $Q(\tilde{\rho}')$ ,  $\tilde{\rho}'=(\rho',\phi')$ , is given by the following integral representations<sup>[4],[5]</sup>:

$$\overline{G}_{s,h}(\bar{\rho},\bar{\rho}',k) = \frac{i}{8} \int_{-\infty}^{\infty} [H_{v}^{(2)}(k\rho_{<}) - \frac{\tilde{Q}H_{v}^{(2)}(ka)}{\tilde{Q}H_{v}^{(1)}(ka)} H_{v}^{(1)}(k\rho_{<})] H_{v}^{(1)}(k\rho_{>}) \exp(iv|\phi - \phi'|) dv \quad (1)$$

where  $\overline{G}_{s,h}$  are the electric and magnetic Green's functions, while  $\rho_{s}$  and  $\rho_{s}$  denote the smaller or larger values of  $\rho$  and  $\rho'$ , respectively. The operator  $\overline{Q}$  is defined as  $\overline{Q} = 1$ 

for the electric case and  $\tilde{Q} = \partial/\partial \rho$  for the magnetic case. The higher-order diffraction terms which reach the observation point P after having encircled the cylinder are omitted in Eq.(1). The  $\exp(-i\omega t)$  time dependence is suppressed.

By applying the Cauchy's residue theorem to the integral in Eq.(1), one may obtain the residue series solution:

$$\overline{G}_{h}(\tilde{\rho}, \tilde{\rho}', k) = \frac{-i}{k a} \sum_{m=1}^{\infty} \left\{ \frac{H_{\mathbf{v}}^{(1)}(k\rho') H_{\mathbf{v}}^{(1)}(k\rho)}{H_{\mathbf{v}}^{(1)}(k a) \frac{\partial}{\partial \nu} H_{\mathbf{v}}^{(1)}(k a)} \exp(i\nu |\phi - \phi'|) \right\}_{\mathbf{v} = \mathbf{v}_{m}}$$
(2)

where the m-th pole  $v_m$  in the complex v-plane is determined from the characteristic equation  $H_{\mathbf{v}}^{(1)}(k \mathbf{a}) = 0$  for the magnetic case. The residue series solution for the electric case is obtained similarly.

When the observation point P is located in the shadow region, the main contribution arises from the poles  $v_m(m=1,2,3...)$  located near v=k a. Thus, one may apply the Debye's approximation<sup>[5]</sup> for the Hankel functions  $H_v^{(1)}(k\rho')$  and  $H_v^{(1)}(k\rho)$  and the Fock-type Airy transition function<sup>[5]</sup> for the Hankel

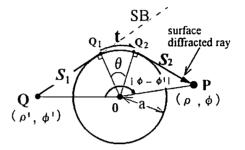


Fig.1 Geometry of the cannonical two-dimensional problem

functions  $H_{\mathbf{v}}^{(1)}(k\,\mathbf{a})$  and  $H_{\mathbf{v}}^{(1)}(k\,\mathbf{a})$  in Eq.(2). Then, by transforming from the complex  $\mathbf{v}$ -plane to the complex  $\tau$ -plane via  $\mathbf{v} = k\,\mathbf{a} + \overline{M}\tau$  where  $\overline{M} = (k\,\mathbf{a}/2)^{1/3}$  and by expanding the phase function in the power of  $\tau^2$ , one may derive the following modified GTD solution.

$$\overline{G}_{h}(\overline{\rho}, \overline{\rho}', k) = \overline{G}(Q_{1}) \left\{ \sum_{m=1}^{\infty} \overline{D}_{m}^{2} \exp(ikt - \overline{\Omega}_{m}t) \overline{A}_{m}^{2} \right\} \overline{G}(Q_{2})$$
(3)

$$\overline{G}(Q_{1,2}) = \frac{i}{4} \sqrt{\frac{2}{\pi k S_{1,2}}} \exp(ikS_{1,2} - i\pi/4), \quad S_1 = \sqrt{(\rho')^2 - a^2}, \quad S_2 = \sqrt{\rho^2 - a^2}$$
 (3a)

$$\overline{D}_{m} = \sqrt{\frac{2M}{\sigma'_{m}}} \frac{\exp(-i\pi/12)}{\operatorname{Ai}(-\sigma'_{m})}, \quad \overline{\Omega}_{m} = \overline{M} \frac{\sigma'_{m}}{a} \exp(-i\pi/6)$$
(3b)

$$\overline{A}_{m} = \exp\left\{\frac{1}{2}\left(\frac{\sigma'_{m}}{2\overline{u}}\right)^{2} \exp(i7\pi/6)\right\}, \quad \overline{u} = \frac{1}{\overline{M}}\sqrt{\frac{kL}{2}}, \quad L = \frac{S_{1}S_{2}}{S_{1} + S_{2}}$$
 (3c)

In obtaining the above solution, we have substituted  $\tau = \sigma'_m \exp(i\pi/3)$  where  $\operatorname{Ai}'(-\sigma'_m) = 0$ . The distance perameters  $S_{1,2}$  and  $t(=a\theta)$  are shown Fig. 1.

One may note that the modified GTD in Eq.(3) is identical to the original GTD proposed by Keller except for the presence of the modification coefficient  $\overline{A}_m$ . The same result has been obtained by Hussar and Albus<sup>[5]</sup>. However, our method is simple and straightforward. It circumvents the complexity associated with their approach.

## 2.2 Three-dimensional problem due to a point source

The three-dimensional Green's function  $G_{s,h}(\tilde{r},\tilde{r}',k)$ , where  $\bar{r}=(\tilde{\rho},z)$  is the observation point,  $\bar{r}'=(\bar{\rho}',z)$  is the source point, and k is the free-space wavenumber, can be obtained from the two-dimensional z independent Green's function  $\overline{G}_{s,h}(\tilde{\rho},\tilde{\rho}',k_l)$  by the following operation:

$$G_{s,h}(\tilde{\mathbf{r}},\tilde{\mathbf{r}}',k) = \frac{1}{2\pi} \int_{-\infty}^{\infty} \overline{G}_{s,h}(\tilde{\mathbf{p}},\tilde{\mathbf{p}}',k_t) \exp(ik_z|\mathbf{z}-\mathbf{z}'|) dk_z, \quad k_t = \sqrt{k^2 - k_z^2}$$
 (4)

The integral in Eq.(4) can be evaluated asymptotically by the saddle point technique<sup>[6]</sup> with the aid of the transformation from the  $k_z$  plane to the  $\psi$  plane via  $k_z = k \sin \psi$ , with  $k_t = k \cos \psi$ . When the two-dimensional modified GTD solution in Eq.(3) is substituted into Eq.(4), the resulting three-dimensional modified GTD solution may be given by the following form:

$$G_{s,h}(\tilde{r},\tilde{r}',k) \sim G(Q_1) \left\{ \sum_{m=1}^{\infty} D_m^2 \exp(ikt - \Omega_m t) A_m^2 \right\} \overline{G}(Q_2) \sqrt{\frac{\overline{S_1}}{\overline{S_1 + t + S_2}}}$$
 (5)

$$G(Q_1) = \exp(ikS_1)/(4\pi S_1), \quad t = \int_{Q_1}^{Q_2} ds$$
 (5a)

The diffraction coefficient  $D_m$ , the attenuation coefficient  $\Omega_m$ , and the modification coefficient  $A_m$  in Eq.(5) are obtained directly from the two-dimensional  $\overline{D}_m$ ,  $\overline{\Omega}_m$ , and  $\overline{A}_m$  in Eqs.(3b) and (3c) by substituting M,  $a(Q_1)$ , and u for  $\overline{M}$ , a, and  $\overline{u}$ , respectively, where M,  $a(Q_1)$ , and u are given by

$$M = (\frac{k \, a}{2})^{1/3}; \quad a(Q_1) = \frac{a}{\cos^2 \psi_s}; \quad u = \sqrt{\frac{kL}{2}}, \quad L = \frac{S_1 S_2}{S_1 + S_2}.$$
 (5b)

The geometrical quantities  $S_1$ , t,  $S_2$ , and  $\psi_s$  are shown in Fig.2. The distance parameters  $S_1'$ , t', and  $S_2'$  in Fig.2 are the projection of  $S_1$ , t, and  $S_2$  on the transverse cross section.  $\psi_s$  corresponds to the departure angle of the spherical wave  $G(Q_1)$  incident on the surface at the point  $Q_1$  at the grazing angle.

## 3. NUMERICAL RESULTS

We implement the numerical calculations to compare the various asymptotic representations involving the GTD, UTD, and modified GTD solutions. As the first example, we have shown in Fig.3 the numerical comparisons of the two-dimensional scattered fields for  $a = 100\lambda$ ,  $\rho' = 110\lambda$ , and  $\rho = 109\lambda$  (see Fig.1). The calculations have been done by moving the observation point P in the  $\phi$  direction.  $|\phi - \phi'| = 48.2^{\circ}$  corresponds to the shadow boundary(SB). The solid curve obtained from the modified GTD (Mod.GTD) in Eq.(3) serves as the reference solution since it agrees excellently with the exact eigenfunction solution<sup>[5]</sup>. The original GTD solution disagrees with the reference solution because the parameter  $\bar{u}$  in Eq.(3c) is 1.23 in this example. Note that the modified GTD in Eq.(3) reduces to the GTD as  $\bar{u} \rightarrow \infty$ . The disagreement between the UTD solution and the reference solution in the deep shadow region is apparent in the figure. Numerical comparisons between the transition term  $\{1 - F[kL\bar{a}]\}/(2\xi\sqrt{\pi})$ ,

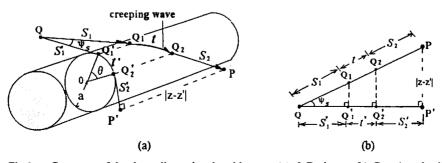


Fig. 2 Geometry of the three-dimensional problem. (a): 3-D view, (b): Developed cylinder.

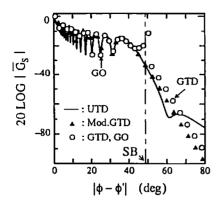


Fig.3 Two-dimensional calculations

where  $F_{[]}$  is the Fresnel integral, and the Pekeris caret function in the UTD formulation<sup>[3],[4]</sup> are shown in Fig.4. It is evident that the transition term (solid curve) is larger than the Pekeris caret function  $\hat{P}_s$  (or  $\hat{P}_h$ ) from the point A (or B) for the electric (or magnetic) case. This is the reason why the UTD formulation does not reduce to the GTD in the deep shadow region.

In Fig.5, we calculated the scattered fields by moving the observation point P to the z direction (see Fig.2). The angle  $\theta$  in Fig.2 is kept constant at 5°. As the observation points move to the z direction, the GTD and UTD solutions deviate

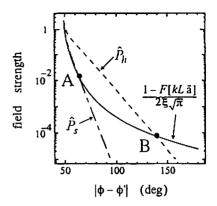


Fig.4 Numerical investigation of UTD

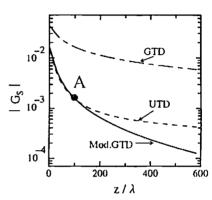


Fig.5 Three-dimensional calculations

from the three-dimensional modified GTD solution calculated from Eq.(5). The reason for these disagreement can easily be found by examining the parameter u in Eq.(5b), and the transition term containing the Fresnel integral and the Pekeris caret function in the three-dimensional UTD formulation.

## 4. CONCLUSION

In the present study, we have derived the two-dimensional modified GTD solution from the exact residue series solution by the simple asymptotic approach. The result has been extended to the three-dimensional modified GTD solution. Numerical comparisons have shown the applicability of the various asymptotic representations involving the GTD, UTD, and modified GTD solutions.

#### References

- [1] J. B. Keller: J. Opt. Soc. Am., Vol. 52, No. 2, pp. 116-130(1962).
- [2] J. B. Keller: IRE Trans. Antennas Propag., Vol. AP-24, pp.312-321(1956).
- [3] P. H. Pathak, W. D. Burnside, and R. J. Marhefka: IEEE Trans. Antennas & Propag., Vol.AP-28, pp.631-642(1980).
- [4] P. H. Pathak: Radio Science, Vol.14, No3, pp.419-435(1979).
- [5] P. Hussar and R. Albus: IEEE Trans. Antennas & Propag., Vol.39, No.12, pp.1672-1680(1991).
- [6] T.Sugihara and T.Ishihara: Tech. Rep., IEE Japan, No.EMT-95-80, pp.167-174, Dec.1995(in Japanese).